

# Trapping and adsorption of CO<sub>2</sub> in amorphous ice: A FTIR study

Óscar Gálvez\*, Belén Maté, Víctor J. Herrero, Rafael Escribano

Instituto de Estructura de la Materia, CSIC, Serrano 121–123, 28006, Madrid, Spain

## ARTICLE INFO

### Article history:

Received 12 February 2008

Revised 30 April 2008

Available online 6 June 2008

### Keywords:

Ices

Ices, IR spectroscopy

Satellites, surfaces

Thermal histories

Comets, composition

## ABSTRACT

The interaction of carbon dioxide and amorphous water ice at 95 K is studied using transmission infrared spectroscopy. Samples are prepared in two ways: co-deposition of the gases admitted simultaneously or sequential deposition, in which amorphous water ice (ASW) is grown first and CO<sub>2</sub> vapor is added subsequently. In either case, a fraction of the CO<sub>2</sub> molecules is found to interact with water in a way that gives rise to shifts and splittings in the infrared bands with respect to those of a pure CO<sub>2</sub> solid. In co-deposition experiments, a larger amount of carbon dioxide is trapped within the amorphous water than in sequential deposition samples, where a substantial proportion of molecules appears to be trapped in macropores of the ASW. The specific surface area of sequential samples is evaluated and compared to previous literature results. When the sequential samples are heated to 140 K, beyond the onset temperature at which water ice undergoes a phase transition, the CO<sub>2</sub> molecules at the pores relocate inside the bulk in a structure similar to that found in co-deposited samples, as deduced by changes in the shape of the CO<sub>2</sub> infrared bands.

© 2008 Elsevier Inc. All rights reserved.

## 1. Introduction

Amorphous water ice, commonly referred to as amorphous solid water (ASW), is a metastable form of ice and the most abundant component of the molecular ices observed in the interstellar medium (Williams et al., 2007). Although ASW has been studied for many years, there are often discrepancies among the diverse literature results describing its physical properties. In particular, disagreement appears in the published values of specific surface area (total surface area divided by the mass of the solid), SSA, with values ranging from 10 to more than 200 m<sup>2</sup>/g reported in different works (see e.g. discussions in Mayer and Pletzer, 1986, or Manca et al., 2003). Temperature values of phase conversion of ASW to cubic ice also show large discrepancies. For example Hagen et al. (1981) give a value around 130 K, Bar-Nun et al. (1987) ~140 K, Boxe et al. (2007) 150 K, and Kumi et al. (2006) around 155 K. Such differences are due to the fact that the amorphous ice properties depend on the way the ice is prepared: e.g. growing conditions or thermal history (Kimmel et al., 2001; Jenniskens and Blake, 1994).

Different molecules such as CO, CO<sub>2</sub>, CH<sub>3</sub>OH, NH<sub>3</sub>, CH<sub>4</sub>, etc., are often present in the ASW found in space (e.g. Dartois, 2005; Gerakines et al., 2005 and references therein). Mixed ices of CO<sub>2</sub> and water are known to be present, for example, in the frozen nuclei of comets (Crovisier, 2006a, 2006b), in various satellites of our Solar System (e.g. Grundy et al., 2003; Buratti et al., 2005),

and as components of dust interstellar particles (e.g. Strazzulla et al., 1998; Draine, 2003). Prompted by these findings, solid H<sub>2</sub>O/CO<sub>2</sub> ice mixtures, as laboratory analogues of astrophysical objects, have been studied for many years, mainly by infrared spectroscopy and mass spectrometry, in temperature programmed desorption (TPD) experiments (see e.g. Sandford and Allamandola, 1990; Ehrenfreund et al., 1999; Bernstein et al., 2005; Kumi et al., 2006; Malyk et al., 2007). In two recent publications (Gálvez et al., 2007; Maté et al., 2008), our group has presented FTIR transmission and reflection-absorption (RAIR) spectra of ices of CO<sub>2</sub> and water prepared by sequential deposition or co-deposition of these species, detecting spectral variations which may characterize two different structures or kinds of association between carbon dioxide and water, either of which may be dominant depending on the temperature and deposition scheme. These spectral variations have been observed before in investigations carried out under different conditions (Sandford and Allamandola, 1990; Kumi et al., 2006). The two different CO<sub>2</sub> structures have been labeled (Maté et al., 2008; Gálvez et al., 2007) CO<sub>2</sub>-ext and CO<sub>2</sub>-int, for external and internal, respectively. The meaning of these terms is the following: in CO<sub>2</sub>-ext the interaction between CO<sub>2</sub> and water is quite weak, as it would be if CO<sub>2</sub> were superficially adsorbed, for instance, whereas by internal it is meant that the CO<sub>2</sub> molecules enter the bulk of ASW. It was found in these studies that CO<sub>2</sub>-ext in a H<sub>2</sub>O/CO<sub>2</sub> ice mixture presents some similar characteristics to those of a pure CO<sub>2</sub> crystal. Both desorb at nominal temperatures around 90–110 K and show a strong peak in the IR spectra at ~2343–2344 cm<sup>-1</sup> at 80 K (Gálvez et al., 2007). On the other hand, CO<sub>2</sub>-int displays a specific behavior in some physical proper-

\* Corresponding author. Fax: +34 91 5855184.

E-mail address: ogalvez@iem.cfmac.csic.es (Ó. Gálvez).

ties, which indicate that in this case the CO<sub>2</sub> molecules are subject to different intermolecular interactions than those present in a pure CO<sub>2</sub> crystal. The desorption of CO<sub>2</sub>-int is entirely controlled by the ASW, taking place between 155 and 168 K, the interval where faster crystallization rates from ASW to I<sub>c</sub> have been observed (Jenniskens and Blake, 1994). The major peak in the FTIR spectra is shifted to  $\sim 2340\text{ cm}^{-1}$ , a lower frequency than that of pure CO<sub>2</sub> or CO<sub>2</sub>-ext.

As mentioned above, two previous papers of our group presented investigations on the carbon dioxide/water system from different points of view and methodology. Gálvez et al. (2007) used transmission IR spectroscopy and TPD experiments to characterize the existence of the two CO<sub>2</sub> structures indicated above, giving also activation energies for the desorption of CO<sub>2</sub> from amorphous and crystalline water ice. In a further work, Maté et al. (2008) employed RAIR spectroscopy to study the morphology and temperature alterations of samples generated by four different deposition techniques, and performed theoretical calculations of a pure CO<sub>2</sub> crystal, with a comparison of theoretical and experimental results. In the present work, we focus on the growing process of CO<sub>2</sub>-int in H<sub>2</sub>O/CO<sub>2</sub> ice mixtures and its dependence on temperature and deposition procedure of CO<sub>2</sub>. We quantify the amount of CO<sub>2</sub>-int formed by codeposition and sequential deposition schemes, and provide a value for the specific surface area of ASW at 95 K using CO<sub>2</sub> as probe molecule, for the first time within our knowledge. Also, we carry out a study of the temperature evolution of these systems in the range between 95 and 165 K, providing evidence on changes in the CO<sub>2</sub> distribution in ASW when phase changes take place.

## 2. Experimental section

Our experimental set-up has been described in detail before (Carrasco et al., 2002; Maté et al., 2003; Gálvez et al., 2007). In brief, it consists of a high vacuum cylindrical chamber, evacuated by a turbomolecular pump. The chamber has a liquid nitrogen Dewar flask in contact with a 1 mm thick deposition substrate made of Si. The background pressure in the chamber is usually in the  $10^{-8}$  mbar range. The chamber is coupled to a Fourier transform infrared spectrometer (Bruker Vertex70) through a purged pathway, with KBr windows for the incident and transmitted radiation, which is focused on exit onto a MCT detector. The substrate is mounted on a holder that allows temperature control, with about 1 K accuracy, between 80 and 250 K. Spectra were recorded with a nominal resolution of  $2\text{ cm}^{-1}$  with 512 co-added scans for each spectrum. Controlled flows of CO<sub>2</sub> and water vapor were introduced through independent needle valves to backfill the chamber. Distilled water previously freeze-pump-thawed three times and 99.998% purity CO<sub>2</sub> from Air Liquide were used in all the experiments. The main chamber is coupled, by means of a regulation valve, to a differentially pumped chamber containing an Inficon, Transpector 2 quadrupole mass spectrometer (QMS), which is used to monitor the vapor composition during the deposition process. This additional QMS chamber, already employed in our previous works on the CO<sub>2</sub>/H<sub>2</sub>O system (Gálvez et al., 2007; Maté et al., 2008), is an improvement of our original configuration (Carrasco et al., 2002; Maté et al., 2003), intended to establish a pressure difference of up to two orders of magnitude between the deposition chamber and the QMS chamber. This modification allows the use of the QMS to control the vapor composition even for relatively high deposition pressures like some of those selected in the present work ( $P > 5 \times 10^{-5}$  mbar). During all the experiments, the position of the regulation valve connecting the two chambers was kept fixed. The use of this two-chamber scheme requires a careful calibration of the QMS to avoid problems associated with the different efficiency of the turbomolecular pumps

for molecules with different masses. The calibration of the QMS was performed by correlating absolute pressure values of water or CO<sub>2</sub> in the main chamber, with the corresponding QMS readings at  $m/q = 18$  and  $m/q = 44$ . Absolute pressures were determined from the growing rates of the solid films on the substrates (Maté et al., 2003). The film thickness values, needed for the calculation of the growing rates, can be derived either from absorbance values (Gálvez et al., 2007) in IR transmission experiments, or from interference patterns in reflection-absorption measurements (Maté et al., 2003). In the present work we have simulated our transmission spectra with the optical constants of Toon et al. (1994) for H<sub>2</sub>O and of Ehrenfreund et al. (1997) for CO<sub>2</sub>. The calibration of the QMS remained stable in the course of the current experiments as verified by periodic checks. The relative sensitivity of the QMS (without electron multiplier) for H<sub>2</sub>O and CO<sub>2</sub> was found to correspond roughly to the ratio of the respective ionization cross sections. The estimated error in the absolute pressures is  $\approx 10\%$ . Deposition pressures ranged between approximately  $5 \times 10^{-7}$  and  $5 \times 10^{-5}$  mbar.

Films of H<sub>2</sub>O/CO<sub>2</sub> ice were prepared by sequential deposition and co-deposition of the appropriate vapors on the substrate held at 95 K. This temperature, relevant for Solar System bodies, was chosen for experimental convenience. At this temperature, the CO<sub>2</sub> saturation pressure is in a range suitable to our experimental setup. In this work, the CO<sub>2</sub> pressure at which CO<sub>2</sub>-ext starts to grow in the ice mixtures, i.e. the saturation pressure, is measured as  $4.3 \times 10^{-5}$  and  $6.6 \times 10^{-5}$  mbar in sequential deposition and co-deposition experiments, respectively. The CO<sub>2</sub>/H<sub>2</sub>O ratio in the ice was determined from the transmission infrared spectra. The amount of water deposited can be calculated from the integrated absorbance of the O–H stretching band. The column density of water molecules is obtained by using the band intensity given by Gerakines et al. (1995) for pure water ice at 80 K,  $A = 2.1 \times 10^{-16}\text{ cm/molecule}$ . Although a slight dependence of the OH-stretching band of water ice with CO<sub>2</sub> concentration has been reported in the literature (Öberg et al., 2007), we have neglected that variation due to the small amount of CO<sub>2</sub> present in our ice mixtures, less than 5% in all cases. To determine the number of CO<sub>2</sub> molecules present in the ice we have followed a similar procedure. The integrated absorbance of the  $\nu_3$  band of CO<sub>2</sub> was converted to molecular column density by means of the band intensity,  $A = 7.1 \times 10^{-17}\text{ cm/molecule}$ , given by Gerakines et al. (1995). This value corresponds to a binary ice mixture of H<sub>2</sub>O/CO<sub>2</sub> in a ratio 24:1 at 10 K. The temperature affects ice properties and the  $A$  values could be slightly different at 95 K. Sandford and Allamandola (1990) estimated that the  $A$  value for the  $\nu_3$  band of CO<sub>2</sub> decreases around 0.5% every 14 K temperature rise, which should not affect significantly our results. We have estimated a 5% error in our integrated areas, giving a 7% error in the corresponding  $n_{\text{CO}_2}/n_{\text{H}_2\text{O}}$  ratios ( $n$ : number of molecules).

## 3. Results and discussion

Fig. 1 presents a transmission IR spectrum of a H<sub>2</sub>O/CO<sub>2</sub> co-deposited sample at 95 K with a calculated percentage of CO<sub>2</sub> in water of 4.5%. In addition to the broad O–H stretching, bending and libration bands of water at  $\sim 3230$ , 1650 and  $800\text{ cm}^{-1}$ , respectively, narrow bands corresponding to the  $\nu_3$  and  $\nu_2$  modes of CO<sub>2</sub> are easily recognized at 2340 and  $656\text{ cm}^{-1}$ , respectively. A small peak at  $2275\text{ cm}^{-1}$  can be also observed, assigned to the  $\nu_3$  band of <sup>13</sup>CO<sub>2</sub>. As it was mentioned in our previous studies (Gálvez et al., 2007; Maté et al., 2008), the main spectral features of CO<sub>2</sub>-int in a H<sub>2</sub>O/CO<sub>2</sub> mixture that differ from the spectrum of pure CO<sub>2</sub> crystals are: (1) a red shift of  $\sim 4\text{ cm}^{-1}$  of the  $\nu_3$  band (at  $\sim 2345\text{ cm}^{-1}$  in pure CO<sub>2</sub>); (2) a corresponding shift of  $\sim 7\text{ cm}^{-1}$  of the same band of <sup>13</sup>CO<sub>2</sub> (at  $\sim 2282\text{ cm}^{-1}$  in pure CO<sub>2</sub>); (3) a

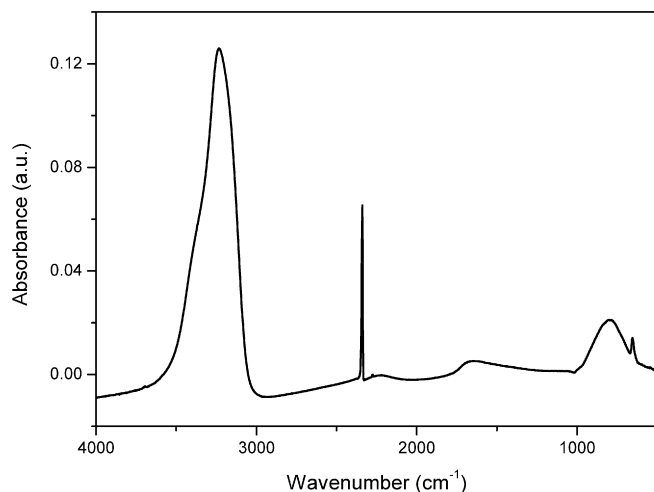


**Fig. 1.** IR spectrum of a co-deposited H<sub>2</sub>O/CO<sub>2</sub> mixture at 95 K in the full mid-IR range recorded.

broad structure in the  $\nu_2$  band (instead of the crystal-field splitting in a pure CO<sub>2</sub> crystal, with a double peak at  $\sim 661$  and  $655$  cm<sup>-1</sup>). These characteristics are visible in the samples analyzed in this study. Table 1 summarizes observed wavenumbers for the vibrational bands of CO<sub>2</sub>-int from spectra of co-deposited CO<sub>2</sub>/H<sub>2</sub>O mixtures, recorded in this work and in previous publications, compared to pure CO<sub>2</sub> values. In the spectral region 3800–3500 cm<sup>-1</sup> only a weak feature at 3696 cm<sup>-1</sup> is observed. This band has been assigned by Roland and Devlin (1991) to the “dangling OH” of ASW. We do not detect any trace of CO<sub>2</sub> combination bands in the spectra of our co-deposited samples at 95 K, in contrast with e.g. the observations by Hodyss et al. (2008) on co-deposited ices grown at 15 K.

### 3.1. Co-deposition experiments

It is important to consider that at 95 K the sticking efficiency of CO<sub>2</sub> molecules on a weakly-interacting substrate like Si is close to zero, whereas the sticking coefficient for water at this temperature is one (Sandford and Allamandola, 1990). In other words, when a CO<sub>2</sub>/H<sub>2</sub>O gas mixture is admitted into the chamber, there is a much lower probability to deposit CO<sub>2</sub> than water, although the presence of water favors the CO<sub>2</sub> condensation. Under these conditions, the presence of CO<sub>2</sub> molecules in the amorphous solid could be explained by the mechanism of gas trapping (e.g. Barnun et al., 2007). The basic idea is that, when water vapor freezes into the ASW structure in the presence of other gases, the guest gas molecules stick to the ice and reside there for a time which depends on the intermolecular interacting forces. If the pores or cavities of ASW are covered by additional water molecules before

the guest gas molecules can escape, they remain trapped and can be released only upon a phase change of the solid.

The H<sub>2</sub>O:CO<sub>2</sub> ratio of the ice mixtures can be varied by choosing different partial pressures of the gases during the co-deposition. We have selected in this investigation water pressures between  $3.2 \times 10^{-6}$  and  $1.6 \times 10^{-5}$  mbar, and CO<sub>2</sub> pressures between  $3.2 \times 10^{-7}$  and  $4.7 \times 10^{-5}$  mbar. Working at constant water vapor pressure, ices were formed by varying the CO<sub>2</sub> pressure. Deposition times ranged between five and twenty minutes leading to ice thickness between 100 and 370 nm. Fig. 2a shows the molecular ratio,  $n_{\text{CO}_2}/n_{\text{H}_2\text{O}}$ , in the ice mixture versus the CO<sub>2</sub> pressure, at constant  $p_{\text{H}_2\text{O}}$ . The  $n_{\text{CO}_2}/n_{\text{H}_2\text{O}}$  ratio is estimated from the spectra as indicated above. The maximum CO<sub>2</sub> concentration was 5%, corresponding to the highest CO<sub>2</sub>-int pressure represented in Fig. 2. At higher pressures CO<sub>2</sub>-ext begins to grow and the resulting ice samples have not been considered in the present study.

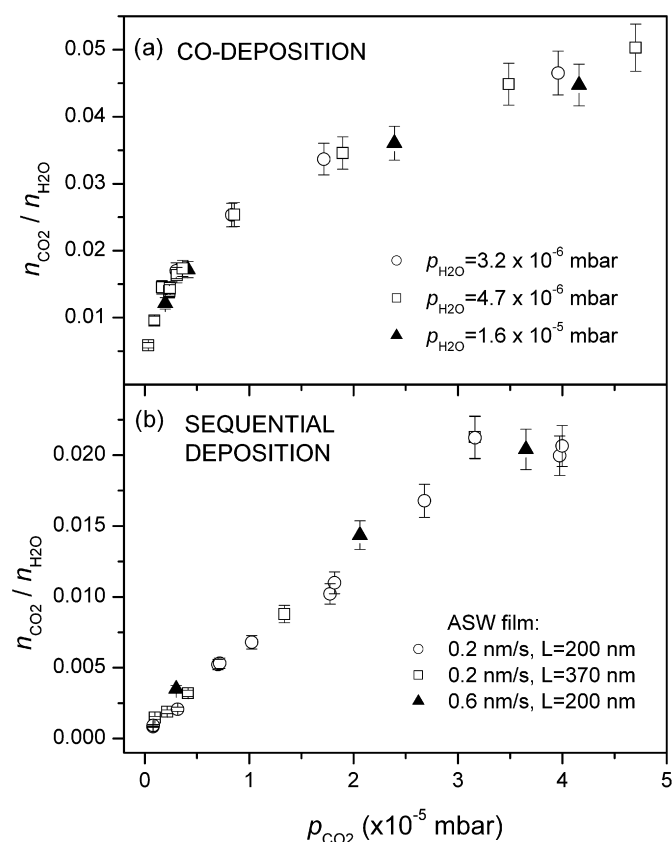


**Fig. 2.** Number of molecules ratio,  $n_{\text{CO}_2}/n_{\text{H}_2\text{O}}$  vs partial CO<sub>2</sub> pressure. (a) Co-deposited ice mixtures for three water pressure values. (b) Sequentially deposited ice mixtures for ASW films of the specified growing rate and thickness.

**Table 1**  
Assignment and positions of CO<sub>2</sub> bands

Assignment	Codeposited (this work, 95 K)	Codeposited (other works)			Pure CO <sub>2</sub> (this work, 95 K)	Pure CO <sub>2</sub> (other works)		
		15 K <sup>a</sup>	100 K <sup>b</sup>	15 K <sup>c</sup>		80 K <sup>a</sup>	80 K <sup>b</sup>	60 K <sup>d</sup>
$\nu_1 + \nu_3$		3703	3701	3702	3708	3708	3708	3708
$2\nu_2 + \nu_3$		3593		3592	3600	3600	3600	3600
<sup>12</sup> CO <sub>2</sub> $\nu_3$	2339		2339	2341	2345		2343	2343
<sup>13</sup> CO <sub>2</sub> $\nu_3$	2275	2278	2277	2279	2282	2282	2282	2283
$\nu_2$	655	656	655	654	661 655	660 655	660 655	660 655

<sup>a</sup> Hodyss et al. (2008): H<sub>2</sub>O/CO<sub>2</sub> 4:1 codeposited mixture, and pure CO<sub>2</sub>.

<sup>b</sup> Sandford and Allamandola (1990): H<sub>2</sub>O/CO<sub>2</sub> 5:1 codeposited mixture, and pure CO<sub>2</sub>.

<sup>c</sup> Bernstein et al. (2005): H<sub>2</sub>O/CO<sub>2</sub> 5:1 codeposited mixture.

<sup>d</sup> Gerakines et al. (1995): Pure CO<sub>2</sub> at 15 K and warm-up to 60 K.

In co-deposition experiments, the trapping mechanism should be responsible for the presence of CO<sub>2</sub> in the amorphous ice, as ice formation and trapping are simultaneous processes. As shown in Fig. 2a, the amount of CO<sub>2</sub>-int trapped depends on the partial pressures selected in the gas phase, and a nonlinear dependence with  $p_{\text{CO}_2}$  is observed. However, at very low CO<sub>2</sub> partial pressures ( $<5 \times 10^{-6}$  mbar) the amount of solid CO<sub>2</sub> is approximately proportional to its vapor partial pressure during co-deposition, as it was recently suggested (Malyk et al., 2007). All three series of measurements agree within their estimated uncertainties. However, slightly smaller values are obtained for the highest water pressure (solid triangles in Fig. 2a). This is consistent with the trapping mechanism, as a lower CO<sub>2</sub>:H<sub>2</sub>O ratio is used for the vapors.

### 3.2. Sequential deposition experiments

We have also conducted a series of experiments with sequentially deposited H<sub>2</sub>O/CO<sub>2</sub> ices (see Fig. 2b). Films of ASW were grown at 95 K and then exposed to different CO<sub>2</sub> partial pressures, in all cases lower than the saturation value of  $4.3 \times 10^{-5}$  mbar, at which CO<sub>2</sub>-ext starts to grow in these experiments. The CO<sub>2</sub> pressure was maintained for a few minutes until a constant infrared band was observed in the spectra. Two water deposition rates, 0.2 and 0.6 nm/s, corresponding to pressures of  $5 \times 10^{-6}$  and  $1.6 \times 10^{-5}$  mbar, respectively, were used to form water films of different thickness, always  $<400$  nm. Fig. 2b shows the molecular ratio,  $n_{\text{CO}_2}/n_{\text{H}_2\text{O}}$ , versus partial pressure of CO<sub>2</sub>, for three series of experiments. All three sets of data coincide within experimental error. The agreement for the results corresponding to the same deposition rate but different ice film thickness (circles and open boxes in Fig. 2b) indicates that the number of CO<sub>2</sub> molecules that enter the solid per gram of water ice is constant. This behavior is in accordance with the conclusions derived by Kumi et al. (2006), who found that the integrated absorbance of the residual  $\nu_3$  band of CO<sub>2</sub> varies linearly with ASW film thickness. The film grown at an approximately three times higher water deposition rate (solid triangles in Fig. 2b) also admits a similar amount of CO<sub>2</sub>-int. This result seems to indicate that the morphology of the ASW does not depend on the deposition rate, at least for the range of values of this work.

These sequential deposition experiments are similar to the standard adsorption isotherm experiments. The data in Fig. 2b follow a tendency that is usually assigned to a type II isotherm, typical of gases physisorbed on a solid (Rouquerol et al., 1999). This kind of isotherm is well described using the Brunauer, Emmet and Teller (BET) model (Brunauer et al., 1938). The BET isotherm model can be formulated as:

$$\frac{p_{\text{CO}_2}}{v(p_{\text{CO}_2}^0 - p_{\text{CO}_2})} = \frac{1}{v_m c} + \frac{c-1}{v_m c} \frac{p_{\text{CO}_2}}{p_{\text{CO}_2}^0}, \quad (1)$$

where  $p_{\text{CO}_2}$  is the actual pressure of CO<sub>2</sub>,  $p_{\text{CO}_2}^0$  the saturation value,  $v$  is the quantity of CO<sub>2</sub> adsorbed per unit mass of water ice, and  $v_m$  the quantity of CO<sub>2</sub> adsorbed per unit mass of water ice for monolayer coverage.  $v$  and  $v_m$  are usually expressed as STP volume of gas (CO<sub>2</sub>) per gram of adsorbent (H<sub>2</sub>O), but they can also be given as the corresponding molecular ratio ( $n_{\text{gas}}/n_{\text{adsorbent}}$ ). The BET constant  $c$  is approximately equal to  $e^{(E_1 - E_L)/kT}$ , where  $E_1$  and  $E_L$  are the heat of adsorption of the first layer and the heat of condensation, respectively. In Fig. 3a we have plotted  $p_{\text{CO}_2}/(v(p_{\text{CO}_2}^0 - p_{\text{CO}_2}))$  versus  $p_{\text{CO}_2}/p_{\text{CO}_2}^0$  for the same experimental data shown in Fig. 2b. A linear fit of the data presented in Fig. 3a has been carried out in the range  $0.01 < p_{\text{CO}_2}/p_{\text{CO}_2}^0 < 0.7$ , as shown in Fig. 3b. This relative pressure interval is consistent with the usual range in which the BET equation is relevant (Rouquerol et al., 1999). The parameters obtained from the fit are collected in Table 2.

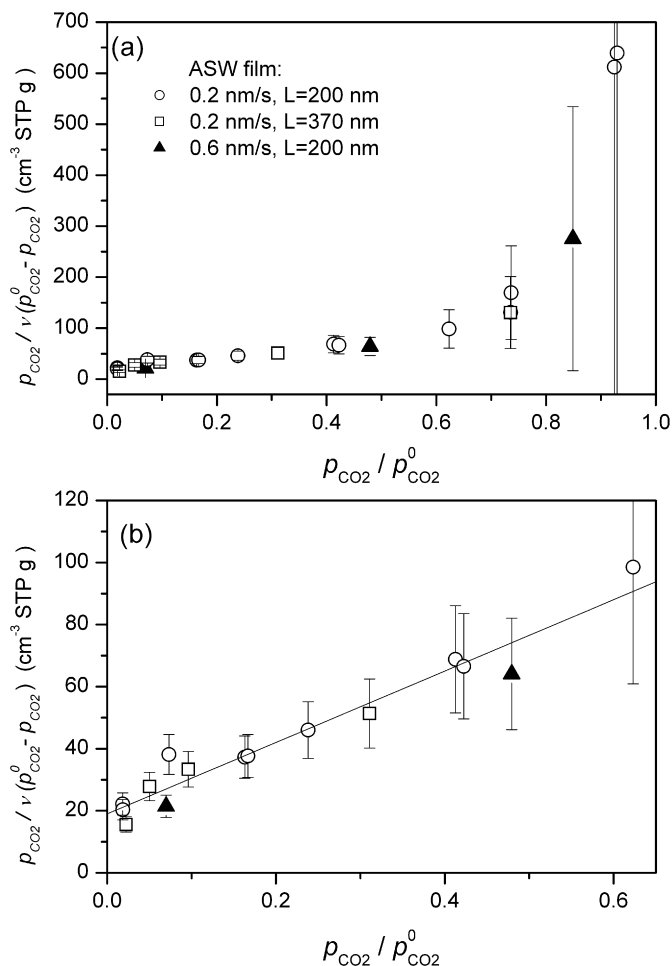


Fig. 3. (a) BET representation of the same experimental data shown in Fig. 2b. (b) Zoomed-in region of  $p_{\text{CO}_2}/p_{\text{CO}_2}^0 < 0.6$ . Solid line: linear fit.

Table 2

BET constant  $c$ ,  $v_m$  expressed as molecular ratio ( $n_{\text{CO}_2}/n_{\text{H}_2\text{O}}$ ), specific surface area SSA ( $\text{m}^2 \text{ g}^{-1}$ ), and net heat of adsorption  $(E_1 - E_L)/k$  (K)

$c$	$v_m$	SSA <sup>a</sup>	$(E_1 - E_L)/k$
7.06	0.0074	39	186

<sup>a</sup> SSA calculated using an estimated cross-sectional area for CO<sub>2</sub> of  $15.5 \text{ \AA}^2$  (see text).

The specific surface area can be derived from  $v_m$  by assuming an effective mean area for the adsorbed CO<sub>2</sub> molecules. We have taken  $15.5 \text{ \AA}^2$  for this magnitude, a value which has been previously used by Sandford and Allamandola and can be obtained from crystallographic data (Simon and Peters, 1980). With this assumption, a SSA of  $39 \pm 15 \text{ m}^2/\text{g}$  for our ASW ice deposited at 95 K has been estimated.

The only other isotherm experiments that we are aware of, in which the concentration of the probe gas molecule in the solid is determined from IR spectra, are those of Manca and co-workers (Manca et al., 2000, 2004; Martin et al., 2002). As in the present case, they employed the integrated absorbance of selected infrared bands of the IR spectrum of the ice to measure the amount of gas adsorbed. They found that this method gives similar results to standard volumetric experiments. Many other isotherm experiments based on volumetric measurements have been published in the literature, although the use of CO<sub>2</sub> as probe gas for ASW has not been reported so far, again within the limit of our knowledge. A study of CO<sub>2</sub> adsorption on water ice, carried out



by Ocampo and Klinger (1982), was performed on hexagonal ice at temperatures between 195 and 273 K. Ghormley (1967) made isotherm experiments on ASW with N<sub>2</sub>, Ar, CH<sub>4</sub>, and O<sub>2</sub>. He obtained for N<sub>2</sub> isotherms a value of 241 m<sup>2</sup>/g at 77 K. Bar-Nun et al. (1987), using Ar as probe gas, found values from 86 m<sup>2</sup>/g at 77 K to 38 m<sup>2</sup>/g at 120 K. Mayer and Pletzer (1986) derived a SSA value of 43.84 m<sup>2</sup>/g at 77 K and of 40 m<sup>2</sup>/g at 113 K from N<sub>2</sub> adsorption measurements. Using also N<sub>2</sub>, Schmitt et al. (1987) found SSA values between 258 and 35 m<sup>2</sup>/g. The infrared and volumetric co-measurements by Manca et al. (2003) were carried out on water ices deposited with Ar at 40 K, then annealed to 90 K to evaporate the Ar, and finally cooled down to the temperature of the experiment. They obtained SSA values of 102.4 m<sup>2</sup>/g for N<sub>2</sub> at 56 K and CO at 57 K, 85 m<sup>2</sup>/g for CH<sub>4</sub> at 73 K, 60.5 m<sup>2</sup>/g for Ar at 60 K, and 40.5 m<sup>2</sup>/g for Kr at 78 K. Their results show a remarkable dependence of the SSA with the probe gas, N<sub>2</sub> and CO giving the largest values both of the *c* BET constant and of the SSA. These observations are consistent with the existence of a specific interaction between the gas molecule and the ice surface leading to a higher affinity with the ice. Hydrogen bonding between ice and adsorbate should contribute to the high value of the adsorption energy, but there is probably another contribution, considering that N<sub>2</sub> and CO are the only molecules in the series studied that have a quadrupole moment. Since CO<sub>2</sub> also has a quadrupole moment, its behavior could be probably closer to that of N<sub>2</sub> or CO than to the rest of the molecules. However, other authors like Schmitt et al. (1987) obtained for N<sub>2</sub> a smaller SSA value than for Ar, in contradiction with the results of Manca et al. (2003). In a recent work Boxe et al. (2007) investigated the dependence of the SSA with water ice temperature using Kr adsorption experiments. They made also a careful study of the dependence of the SSA with the H<sub>2</sub>O deposition rate and ice mass and concluded that the SSA is independent of both magnitudes, within their experimental error limits. They reported SSA values of  $102.3 \pm 26.8$  m<sup>2</sup>/g at 83.5 K, and  $52.47 \pm 14.98$  m<sup>2</sup>/g at 101 K.

Despite the disparity of methods and SSA values commented on in the previous paragraph there is a clear tendency to the decrease of SSA with growing ice temperature. The value of  $39 \pm 15$  m<sup>2</sup>/g at 95 K obtained in this work is consistent with some of the results previously mentioned, like those of Mayer and Pletzer (1986), Bar-Nun et al. (1987) and Boxe et al. (2007). In a previous publication (Gálvez et al., 2007), we provided a rough estimate of 140–280 m<sup>2</sup>/g for ASW ice at 85 K. This value is probably overestimated, since the crude assumptions made in that work do not allow for a proper distinction between mono- and multilayer adsorptions. In the present case, our SSA value arising from the application of the BET model corresponds to monolayers exclusively.

### 3.3. Comparison between co-deposition and sequential deposition methods

An inspection of the two panels in Fig. 2 provides an immediate comparison between the two types of deposition employed in this work. In both cases, the measurements were performed at 95 K and with similar pressure ranges for CO<sub>2</sub> and H<sub>2</sub>O. The different ordinate scale reveals that there is always more CO<sub>2</sub> present in the co-deposited samples, with a  $n_{\text{CO}_2}/n_{\text{H}_2\text{O}}$  ratio between nine times (at  $p_{\text{CO}_2} \sim 1 \times 10^{-6}$  mbar) and 2.3 times (at  $p_{\text{CO}_2} \sim 4 \times 10^{-5}$  mbar) larger. If the data in Fig. 2a is plotted as a BET isotherm, the value for the surface active area is about three times higher than that evaluated for sequentially deposited experiments.

It is also interesting to remark that the maximum CO<sub>2</sub> pressure at which CO<sub>2</sub>-ext starts to grow is smaller in the sequential deposition than in the co-deposition scheme ( $4.3 \times 10^{-5}$  versus  $6.6 \times 10^{-5}$  mbar, respectively).

### 3.4. Spectral band shape

In the following paragraphs the different band shapes of the CO<sub>2</sub>  $\nu_3$  band observed in both experiments will be discussed in an attempt to clarify the CO<sub>2</sub>–H<sub>2</sub>O interactions in these ice mixtures.

The  $\nu_3$  band adopts different shapes for sequential and co-deposition experiments at 95 K. Thinner and more symmetric bands are obtained in co-deposited samples. This band shape is typical of gas-phase spectra or of molecules isolated in a homogeneous solid matrix, which could be similar to our co-deposited samples, composed by CO<sub>2</sub> molecules trapped in a water surrounding.

In sequential deposition, the porous structure of the ASW formed is the key property in the process of gas adsorption. This porous structure is still under debate. From their isotherm experiments at 77 K Mayer and Pletzer (1986) concluded that ASW was microporous. They compared their experimental isotherm with a nonporous standard isotherm, which they selected as the isotherm obtained from ASW deposited at 113 K. This empirical method, the so-called “ $\alpha$ -plot,” allows a semi-quantitative analysis of the microporosity of the material. If the sample is nonporous, adsorptions are similar on both materials (sample and reference) and the adsorbed amounts are proportional. Conversely, for a microporous sample, deviation from linearity at the beginning of adsorption is observed. In more recent works Manca and co-workers (Manca et al., 2000, 2002) have shown that the  $\alpha$ -plots depend on the probe molecule used; this implies that the analysis has to be done with caution. In their studies, they claimed that their ASW samples, formed by a different deposition process than that used by Mayer and Pletzer, were nonmicroporous, arguing that the high SSA obtained was due to the formation of micro grains. In the last years, different studies have appeared in the literature concerning this topic. For example, Raut et al. (2007) have confirmed that the porosity of the ASW samples can be strongly altered by simply changing the angle of deposition in a collimated water vapor beam, in agreement with previous studies (Stevenson et al., 1999; Kimmel et al., 2001). Discrepancies in the different results found in the literature stress the fact that the porosity of the ASW is highly dependent on the way the ice is generated.

The broader bands observed in our sequential samples are symptomatic of CO<sub>2</sub> molecules in an inhomogeneous environment, undergoing intermolecular interactions of different strength, which results in IR absorptions spanning a wide frequency range. This could be the case for interactions occurring in a rough or macroporous surface, as opposed to the microporosity hypothesis in which a more homogeneous environment surrounding the CO<sub>2</sub> molecules is expected. The diameter of the cavity or macropore in the water ice is large enough to contain tens of layers of CO<sub>2</sub>. Due to the constraint given by the confinement to the shape of these cavities, the formation of a highly ordered structure of CO<sub>2</sub> is hindered. This fact induces broader IR bands, typical of an amorphous solid. The relatively small SSA obtained in this work (see Table 1) supports also the macroporous hypothesis. The macropores can also be understood as inter-grain cavities in the ice (Boxe et al., 2007).

In a typical sequential experiment, the intensity of the CO<sub>2</sub>-int  $\nu_3$  band starts to decrease just after the CO<sub>2</sub> leak valve is closed. After a few minutes, which depend of the initial  $p_{\text{CO}_2}$  of the experiment, a constant integrated band value is observed, indicating that the desorption of CO<sub>2</sub> molecules from the ice has ceased. Further warming the ice to 105 K does not change the integrated band intensity. This band persists until the phase transition to the crystalline cubic structure, *I<sub>c</sub>*, is nearly completed, at  $\sim 160$  K, as was observed before (Jenniskens and Blake, 1994). Although the integrated band area remains constant, the shape of the band is significantly altered from 105 to 140 K (see Fig. 4a). At  $\sim 131$  K the ASW undergoes a phase transition from the low-density amor-

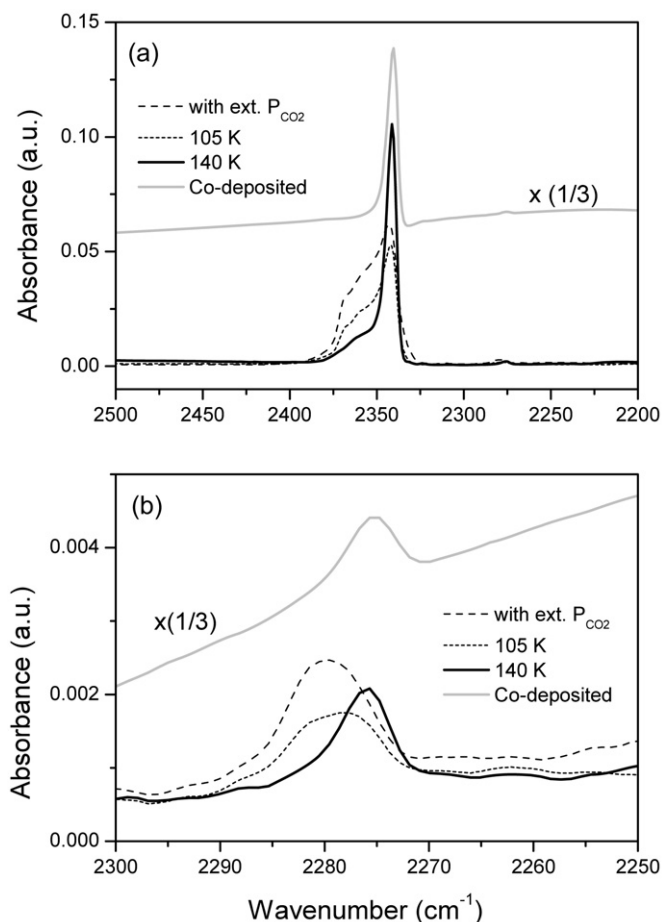


**Fig. 4.** (a) FTIR spectra of the  $\nu_3$  band of  $\text{CO}_2$  in co-deposited and sequentially deposited ice mixtures with the same water amount. Gray solid line: Co-deposited  $\text{CO}_2/\text{H}_2\text{O}$  ice. The spectrum has been scaled by a factor (1/3) and offset for clarity. Dashed line: Spectrum taken after 14 min of exposure of a 370 nm ASW film to a  $\text{CO}_2$  pressure of  $3.2 \times 10^{-5}$  mbar. Dotted line: Spectrum taken after stopping the  $\text{CO}_2$  flow and warming the ice to 105 K. Black solid line: Spectrum taken after warming the ice to 140 K. (b) Zoomed-in spectra in the  $\nu_3$  region of  $^{13}\text{CO}_2$ .

phous structure,  $I_{a1}$ , to a third amorphous form,  $I_{a1r}$ , which precedes the crystallization to cubic ice,  $I_c$ , and coexists metastably with  $I_c$  in a wide range of temperatures (Jenniskens and Blake, 1994). During this phase transition, water molecules are rearranged and  $\text{CO}_2$  molecules are free to move through the canals and pathways temporarily formed during this process. As a result,  $\text{CO}_2$  molecules are diluted inside the amorphous water structure in a way that, based on the band shape resemblance (see gray and solid black lines in Fig. 4a), is closer to that present in co-deposition experiments. Panel (b) of Fig. 4 presents zoomed-in spectra in the  $\nu_3$  region of  $^{13}\text{CO}_2$ . At 140 K the band peak position has shifted from  $\sim 2280$  to  $\sim 2275 \text{ cm}^{-1}$ , which coincides with the frequency observed for co-deposited samples, and supports the assumption that at 140 K the  $\text{CO}_2$  molecular environment for sequentially deposited samples becomes similar to that in co-deposited samples at 95 K.

The  $c$  BET constant gives an idea of the strength of the  $\text{CO}_2$ – $\text{H}_2\text{O}$  interaction (responsible for the formation of the monolayer) as compared to the  $\text{CO}_2$ – $\text{CO}_2$  interaction (responsible for the condensation process). From sequential experiments we have obtained a  $(E_1 - E_L)/k$  value of  $186 \pm 50 \text{ K}$ . This value is consistent with the difference of 170 K between the heats of desorption of  $\text{CO}_2$ – $\text{H}_2\text{O}$  ( $2860 \pm 200 \text{ K}$ ) and  $\text{CO}_2$ – $\text{CO}_2$  ( $2690 \pm 200 \text{ K}$ ) reported by Sandford and Allamandola (1990), but the coincidence is not conclusive due to the large uncertainties in the values of those magnitudes.

## 4. Conclusions

The formation of  $\text{CO}_2$ -int in  $\text{H}_2\text{O}/\text{CO}_2$  ice mixtures generated at 95 K by two different procedures, sequential deposition and co-deposition, has been studied in detail, yielding some quantitative results. These ice mixtures are abundant in different astrophysical bodies, and this study should help in the exploration of the physical properties of these objects. The main features obtained in this work are summarized below.

The mechanism of formation of  $\text{CO}_2$ -int depends on the procedure of deposition of the gases. In a co-deposited mixture, molecules of  $\text{CO}_2$  are trapped in the amorphous water ice as it grows. The number of trapped molecules is not proportional to the  $\text{CO}_2$  vapor pressure, but its growth rate decreases with increasing  $\text{CO}_2$  proportion. The shape of the  $\nu_3$  IR band suggests that the  $\text{CO}_2$  molecules in these samples are located in a homogeneous environment. On the other hand, in sequentially deposited mixtures, the  $\text{CO}_2$  molecules are filling the pores of the ASW, forming multilayers. For the  $\text{CO}_2$  and  $\text{H}_2\text{O}$  vapor pressure ranges studied in this work, between nine and 2.3 times more  $\text{CO}_2$ -int is formed in co-deposited than in sequentially deposited samples.

From sequential deposition experiments, we have estimated for ASW at 95 K a SSA of  $39 \pm 15 \text{ m}^2/\text{g}$ , which falls within the widely spread literature data. This small SSA value, together with the band shape deformation observed for the  $\text{CO}_2$   $\nu_3$  band, favors the evidence that we have grown a macroporous ASW.

Annealing the sequentially deposited ice mixtures to 140 K entails a water phase transition. In this process the  $\text{CO}_2$  molecules, located inside the pores in sequentially deposited samples, rearrange in the water structure reaching a  $\text{CO}_2$  distribution equivalent to that in co-deposited samples.

The different signatures of the IR spectra of  $\text{CO}_2$  trapped and adsorbed in amorphous water can be relevant for the interpretation of spectra of cometary nuclei, when they become available. The heating of the nuclei when comets pass by their perihelion may induce redistribution of the  $\text{CO}_2$  molecules in the ice as described above, with consequent effects that can be detected by IR spectroscopy of sufficient quality. For instance, the spectra taken before and after impact on Comet 9P/Tempel 1 by the Deep Impact probe, shown in Fig. 7 of Crovisier (2006a), reveal a change in the region of the  $\nu_3$  band of  $\text{CO}_2$ , with a shoulder growing on the low-frequency side of the band. However, the quality of the spectra is not sufficient to allow for an unambiguous assignment of this feature. It can be expected that the data supplied in the present investigation could help to unravel observational data in the future.

## Acknowledgments

This research has been carried out with funding from the Spanish Ministry of Education, Projects FIS2004-00456 and FIS2007-61686. O.G. acknowledges financial support from the same Ministry, “Juan de la Cierva” program.

## References

- Bar-Nun, A., Dror, J., Kochvi, E., Laufer, D., 1987. Amorphous water ice and its ability to trap gases. *Phys. Rev. B* 35 (5), 2427–2435.
- Bar-Nun, A., Notoescu, G., Owen, T., 2007. Trapping of  $\text{N}_2$ , CO and Ar in amorphous ice—Application to comets. *Icarus* 190, 655–659.
- Bernstein, M.P., Cruikshank, D.P., Sanford, S.A., 2005. Near-infrared laboratory spectra of solid  $\text{H}_2\text{O}/\text{CO}_2$  and  $\text{CH}_3\text{OH}/\text{CO}_2$  ice mixtures. *Icarus* 179, 527–534.
- Boxe, C.S., Bodsgard, B.R., Smythe, W., Leu, M.T., 2007. Grain sizes, surface areas, and porosities of vapor-deposited  $\text{H}_2\text{O}$  ices used to simulate planetary icy surfaces. *J. Colloid Interface Sci.* 309, 412–418.
- Brunauer, S., Emmett, P.H., Teller, E., 1938. Adsorption of gases in multimolecular layers. *J. Am. Chem. Soc.* 60, 309–319.
- Burratt, B.J., and 28 colleagues, 2005. Cassini visual and infrared mapping spectrometer observations of Iapetus: Detection of  $\text{CO}_2$ . *Astrophys. J.* 622 (2), L149–L152.

- Carrasco, E., Castillo, J.M., Escribano, R., Herrero, V.J., Moreno, M.A., Rodríguez, J., 2002. A cryostat for low-temperature spectroscopy of condensable species. *Rev. Sci. Instr.* 73, 3469–3473.
- Crovisier, J., 2006a. Recent results and future prospects for the spectroscopy of comets. *Mol. Phys.* 104 (16–17), 2737–2751.
- Crovisier, J., 2006b. New trends in cometary chemistry. *Faraday Discuss.* 133, 375–385.
- Dartois, E., 2005. The ice survey opportunity of ISO. *Space Sci. Rev.* 119, 293–310.
- Draine, B.T., 2003. Interstellar dust grains. *Annu. Rev. Astron. Astrophys.* 41, 241–289.
- Ehrenfreund, P., Boogert, A.C.A., Gerakines, P.A., Tielens, A.G.G.M., van Dishoeck, E.F., 1997. Infrared spectroscopy of interstellar apolar ice analogs. *Astron. Astrophys.* 328, 649–669.
- Ehrenfreund, P., Kerkhof, O., Schutte, W.A., Boogert, A.C.A., Gerakines, P.A., Dartois, E., d'Hendecourt, L., Tielens, A.G.G.M., van Dishoeck, E.F., Whittett, D.C.B., 1999. Laboratory studies of thermally processed H<sub>2</sub>O–CH<sub>3</sub>OH–CO<sub>2</sub> ice mixtures and their astrophysical implications. *Astron. Astrophys.* 350, 240–253.
- Gálvez, O., Ortega, I.K., Maté, B., Moreno, M.A., Martín-Llorente, B., Herrero, V.J., Escribano, R., Gutiérrez, P.J., 2007. A study of the interaction of CO<sub>2</sub> with water ice. *Astron. Astrophys.* 472 (2), 691–698.
- Gerakines, P.A., Schutte, W.A., Greenberg, J.M., van Dishoeck, E.F., 1995. The infrared band strength of H<sub>2</sub>O, CO, and CO<sub>2</sub> in laboratory simulations of astrophysical ice mixtures. *Astron. Astrophys.* 296, 810–818.
- Gerakines, P.A., Bray, J.J., Davis, A., Richey, C.R., 2005. The strengths of near-infrared absorption features relevant to interstellar and planetary ices. *Astrophys. J.* 620, 1140–1150.
- Ghormley, J.A., 1967. Adsorption and occlusion of gases by low-temperature forms of ice. *J. Chem. Phys.* 46 (4), 1321–1325.
- Grundy, W.M., Young, L.A., Young, E.F., 2003. Discovery of CO<sub>2</sub> ice and leading-trailing spectral asymmetry on the uranian satellite Ariel. *Icarus* 162, 222–229.
- Hagen, W., Tielens, A.G.G.M., Greenberg, J.M., 1981. The infrared spectra of amorphous solid water and ice, I<sub>c</sub>, between 10 K and 140 K. *Chem. Phys.* 56, 367–379.
- Hodyss, R., Johnson, P.V., Orzechowska, G.E., Goguen, J.D., Kanik, I., 2008. Carbon dioxide segregation in 1:4 and 1:9 CO<sub>2</sub>:H<sub>2</sub>O ices. *Icarus* 194, 836–842.
- Jenniskens, P., Blake, D.F., 1994. Structural transitions in amorphous water ice and astrophysical implications. *Science* 265, 753–756.
- Kimmel, G.A., Stevenson, K.P., Dohnálek, Z., Smith, R.S., Kay, B.D., 2001. Control of amorphous solid water morphology using molecular beams. I. Experimental results. *J. Chem. Phys.* 114 (12), 5284–5294.
- Kumi, G., Malyk, S., Hawkins, S., Reisler, H., Wittig, C., 2006. Amorphous solid water films: Transport and guest–host interactions with CO<sub>2</sub> and N<sub>2</sub>O dopants. *J. Phys. Chem. A* 110, 2097–2105.
- Malyk, S., Kumi, G., Reisler, H., Witting, C., 2007. Trapping and release of CO<sub>2</sub> guest molecules by amorphous ice. *J. Phys. Chem. A* 111, 13365–13370.
- Manca, C., Roubin, P., Martin, C., 2000. Volumetric and infrared co-measurements of CH<sub>4</sub> and CO isotherms on microporous ice. *Chem. Phys. Lett.* 330, 21–26.
- Manca, C., Martin, D., Roubin, P., 2002. Spectroscopic and volumetric characterization of a non-microporous amorphous ice. *Chem. Phys. Lett.* 364, 220–224.
- Manca, C., Martin, C., Roubin, P., 2003. Comparative study of gas adsorption on amorphous ice: Thermodynamic and spectroscopic features of the adlayer and the surface. *J. Phys. Chem. B* 107, 8929–8941.
- Manca, C., Martin, C., Roubin, P., 2004. Volumetric and infrared measurements on amorphous ice structure. *Chem. Phys.* 300, 53–62.
- Martin, C., Manca, C., Roubin, P., 2002. Adsorption of small molecules on amorphous ice: Volumetric and FT-IR isotherm co-measurements. Part I. Different probe molecules. *Surface Sci.* 502–503, 275–279.
- Maté, B., Medialdea, A., Moreno, M.A., Escribano, R., Herrero, V.J., 2003. Experimental studies of amorphous and polycrystalline ices films using FT-RAIRS. *J. Phys. Chem. B* 107 (40), 11098–11108.
- Maté, B., Gálvez, O., Martín-Llorente, B., Moreno, M.A., Herrero, V.J., Escribano, R., Artacho, E., 2008. Ices of CO<sub>2</sub>/H<sub>2</sub>O mixtures. Reflection–absorption IR spectroscopy and theoretical calculations. *J. Phys. Chem. A* 112 (3), 457–465.
- Mayer, E., Pletzer, R., 1986. Astrophysical implications of amorphous ice—A microporous solid. *Nature* 319 (23), 298–301.
- Öberg, K.I., Fraser, H.J., Boogert, A.C.A., Bisschop, S.E., Fuchs, G.W., van Dishoeck, E.F., Linnartz, H., 2007. Effects of CO<sub>2</sub> on H<sub>2</sub>O band profiles and band strengths in mixed H<sub>2</sub>O:CO<sub>2</sub> ices. *Astron. Astrophys.* 462, 1187–1198.
- Ocampo, J., Klinger, J., 1982. Adsorption of N<sub>2</sub> and CO<sub>2</sub> on ice. *J. Colloid Interface Sci.* 86 (2), 377–383.
- Raut, U., Famá, M., Teolis, B.D., Baragiola, R.A., 2007. Characterization of porosity in vapor-deposited amorphous solid water from methane adsorption. *J. Chem. Phys.* 127, 204713.
- Roland, B., Devlin, J.P., 1991. Spectra of dangling OH groups at ice cluster surfaces and within pores of amorphous ice. *J. Chem. Phys.* 94, 812–813.
- Rouquerol, F., Rouquerol, J., Sign, K., 1999. Adsorption by Powders & Porous Solids. Academic Press, London.
- Sandford, S.A., Allamandola, L.J., 1990. The physical and infrared spectral properties of CO<sub>2</sub> in astrophysical ice analogs. *Astrophys. J.* 355, 357–372.
- Schmitt, B., Ocampo, J., Klinger, J., 1987. Structure and evolution of different ice surfaces at low temperature. Adsorption studies. *J. Phys. Colloq.* C1 48 (3), 519–525.
- Simon, A., Peters, K., 1980. Single-crystal refinement of the structure of carbon-dioxide. *Acta Crystallogr. B* 36, 2750–2751.
- Stevenson, K.P., Kimmel, G.A., Dohnálek, Z., Smith, R.S., Kay, B.D., 1999. Controlling the morphology of amorphous solid water. *Science* 283, 1505–1507.
- Strazzulla, G., Nisini, B., Leto, G., Palumbo, M.E., Saraceno, P., 1998. Solid CO<sub>2</sub> towards NGC7538 IRS1. *Astron. Astrophys.* 334, 1056–1059.
- Toon, O.B., Tolbert, M.A., Birgit, G.K., Middlebrook, A.M., 1994. Infrared optical constants of H<sub>2</sub>O ice, amorphous nitric acid solutions and nitric acid hydrates. *J. Geophys. Res.* 99 (D12), 25631–25654.
- Williams, D.A., Brown, W.A., Price, S.D., Rawlings, J.M.C., Viti, S., 2007. Molecules, ices and astronomy. *Astron. Geophys.* 48 (1), 25–34.